ELSEVIER

Journal of Contaminant Hydrology 20 (1995) 127–143

JOURNAL OF
Contaminant
Hydrology

Ionic tracer movement through highly weathered sediments

J.C. Seaman [a,*], P.M. Bertsch [a], W.P. Miller [b]

[a] *Savannah River Ecology Lab, Biogeochemistry Division, University of Georgia, Drawer E, Aiken, SC 29802, USA*

[b] *Environmental Soil Science Department, University of Georgia, Athens, GA 30602, USA*

Received 15 December 1994; accepted 8 May 1995 after revision

Abstract

A highly-weathered, sandy aquifer material from the Upper Coastal Plain region of the southeastern U.S.A. (Aiken, South Carolina) was used to determine the impact of ionic strength and solution composition on the determination of physical transport parameters using ionic tracers. The mineralogy of the clay fraction consisted primarily of kaolinite, goethite and mica. Repacked saturated columns (bulk density ~ 1.5 g cm^{-3}) were leached at a constant rate (~ 0.25 cm min^{-1}) with a given tracer solution. For comparison, tritium (~ 200 pCi mL^{-1}) was included in leachate of selected columns and several of the experiments were replicated in columns of acid-washed sand. Pore volume estimates based on tritium breakthrough were consistent with those calculated from the bulk density of the repacked matrix. In contrast, solute breakthrough for the sandy geologic material was dependent on concentration, as well as cation and anion type. At low ionic strengths (0.0005–0.010 *M*) that are analogous to conditions that may be encountered in field-scale transport experiments, neither the cation nor the anion acted conservatively, yielding systematically high estimates of column porosity or low estimates of flow velocity. At the higher ionic strengths (~ 0.10 *M*), solute breakthrough was essentially conservative regardless of ionic composition. The impact of cation valence and concentration on Br^- breakthrough was determined using $MgBr_2$ and KBr solutions of varying concentrations (0.001–0.1 *N*). Bromide breakthrough was substantially delayed for concentrations below 0.10 *M* and was delayed to a greater extent in the presence of a divalent cation (Mg^{2+}) than in the presence of a monovalent cation (K^+). Failure to recognize these interactions in the field could lead to a false interpretation of Br displacement in terms of physical interactions, i.e. flow velocity, dispersivity, etc.

* Corresponding author.

0169-7722/95/$09.50 © 1995 Elsevier Science B.V. All rights reserved
SSDI 0169-7722(95)00043-7

1. Introduction

Hydrologic modeling describes the transport of a nonreactive tracer as a function of mass flow (advection), based on the hydraulic conductivity (K) of the transmissive zone, and a combination of other factors such as diffusion and small-scale variations in flow path and velocity (hydrodynamic dispersion). Transport parameters, such as the pore water velocity (V [L T^{-1}]) and dispersion coefficient (D [L^2 T^{-1}]), are determined by calibration of the advection–dispersion equation to the spatial distribution or breakthrough of a "non-reactive" tracer (Parker and van Genuchten, 1984). An assumption is made that the position of the solute plume is a manifestation of the physical properties of the transmissive zone and not a function of chemical interaction between the tracer and the porous medium.

The basic equation for the transport of an interactive tracer under steady-state water flow conditions in a one-dimensional homogeneous system is:

$$\frac{\rho}{\theta}\frac{\partial S}{\partial t} + \frac{\partial C_r}{\partial t} = D\frac{\partial^2 C_r}{\partial x^2} - V\frac{\partial C_r}{\partial x} \tag{1}$$

where ρ is the bulk density of the porous medium; θ is the volumetric water content; C is the concentration of the compound of interest in the liquid phase; S is the adsorbed concentration per unit mass of solid phase; x is the distance; and t is time. For simplicity of discussion, a linear equilibrium adsorption model:

$$S = kC_r \tag{2}$$

where k is an empirical partitioning constant, will be employed. Substituting the above adsorption term into the transport equation yields:

$$R\frac{\partial C_r}{\partial t} = D\frac{\partial^2 C_r}{\partial x^2} - V\frac{\partial C_r}{\partial x} \tag{3}$$

where R, the dimensionless retardation factor, can be defined as

$$R = 1 + \rho k/\theta \tag{4}$$

Ideally, a non-reactive tracer ($R = 1$) allows the measurement of the transport parameters (V and D) without altering the fluid properties of the groundwater or the surface chemical and transmissive properties of the aquifer matrix. However, when chemical interactions are combined with the physical processes of transport, it becomes difficult to distinguish between a nonlinear adsorption process under the influence of a constant flow gradient, and a linear or pseudo-linear adsorption process under the influence of a more complicated flow regime.

Surface–solute interactions that alter surface charge on the clay mineral fraction can influence the transport of ionic solutes through subsurface systems. Clay minerals can be divided into two basic groups according to the origin of surface charge: (1) constant surface charge minerals; and (2) constant surface potential or variable-charge minerals. Most soils and geologic systems represent hybrids of the two basic groups because they are composed of varying quantities of both mineral types, and because the edges of constant-charge clay minerals display variable charge character. The zero point of net

charge (ZPNC) for a mixed system is the pH at which the anion exchange capacity and the cation-exchange capacity (CEC) are equivalent under a given set of solution conditions (Sposito, 1984).

For variable-charge minerals, surface charge is created by the excess adsorption of the potential determining ions (H^+ and OH^-) at the mineral surface; thus, the sign and magnitude of surface charge can vary with the concentration and activity of these two species. The zero point of charge (ZPC) for a constant potential mineral is the pH at which the total net particle charge vanishes under a given set of solution conditions (Sposito, 1984). Depending on mineral composition and the degree of crystallinity, the ZPC for hydrous Fe- and Al-oxides is generally in the pH range of 7–9 (van Olphen, 1977). Under pH conditions below the ZPC, the mineral will possess a net positive charge; conversely, at pH-values above the ZPC the surface will be negatively charged. In addition, the surface charge density of a variable-charge mineral is a function of: (1) valence of the counter ion; (2) dielectric constant of the solution; (3) temperature; (4) electrolyte concentration; (5) pH of the bulk solution; and (6) the ZPC of the oxide mineral (Uehara and Gillman, 1981). Also, specific adsorption of polyvalent cations or anions at the oxide surface can alter the expression of net surface charge (Stumm and Morgan, 1981; Uehara and Gillman, 1981).

Under most field conditions, bromide and chloride are characterized as "conservative" or "nonreactive" tracers (Freyberg, 1986; Gelhar et al., 1992; Jensen et al., 1993) due to the coarse texture of the groundwater matrix and the assumed presence of constant/negatively charged clay minerals. In many instances this may be a valid assumption. For example, chloride migrated at essentially the same rate ($V = 0.7$ m day^{-1}) as tritium ($V = 0.75$ m day^{-1}) in a sandy aquifer in Denmark, but a greater vertical spreading of the chloride plume was attributed to differences in density between the native groundwater and the more concentrated tracer solution (Jensen et al., 1993). However, the non-conservative ($R \neq 1$) movement of anionic tracers has been well documented in laboratory column studies (McMahon and Thomas, 1974; Chan et al., 1980; Wong et al., 1990; Ishiguro et al., 1992) and has been reported in some field experiments (e.g., Boggs and Adams, 1992). The most often recognized non-conservative interaction ($R < 1$) is anion exclusion, resulting in more rapid tracer movement than can be attributed to water flux (Thomas and Swoboda, 1970; Cameron and Wild, 1982). This interaction is so commonly acknowledged that the definition of a conservative tracer is often expanded to include tracers that move at a rate greater than water flow ($R < 1$).

Although exclusion and adsorption have an opposite effect on the transport velocity of a given ionic species, both are controlled by the expression of surface charge and its neutralization at the solid–solution interface. McMahon and Thomas (1974) found that the degree of anion exclusion compared to tritium increased with increasing CEC of the soil matrix. Thomas and Swoboda (1970) observed that the degree of exclusion in a clayey soil decreased with increasing concentration of the tracer, but they attributed the increase in effective pore volume to the enhanced ability of the anion to diffuse into the clay interlayers rather than a change in the interlayer spacing or physical associations of the clay constituents. In addition to tracer concentration, McMahon and Thomas (1974) observed that the degree of anion exclusion or retardation can be altered by physical

sample disruption that destroyed the natural soil structure or changed the spacial distribution of the clay minerals.

In contrast to anion exclusion, the delayed arrival of Br and Cl has been observed in soils and sediments that contain significant quantities of variable-charge clay minerals (Berg and Thomas, 1959; McMahon and Thomas, 1974; Chan et al., 1980; Boggs and Adams, 1992; Ishiguro et al., 1992). For example, Chan et al. (1980) observed that Cl^- breakthrough in an oxidic soil was dependent on both the pH and ionic strength of the treatment solution. Ishiguro et al. (1992) noted that under fixed ionic strength conditions, Br^- was delayed to a greater extent in an allophanic andisol at low pH-values (~ 4.2), while Sr^{2+} was retarded to a greater extent at high pH-values (~ 7.7). Under intermediate pH conditions (5.6) and low solution concentrations (< 0.01 M), which are analogous to those usually experienced in the field, neither the cation nor the anion behaved conservatively. Because many factors influence surface charge development, the mobility of a solute through porous media containing variable-charge minerals is highly dependent on the exact solution conditions. Such interactions are more clearly recognized by focussing on both ionic species being transported in a cation–anion pair (i.e. KBr, K_2SO_4, etc.).

The objective of this study was to determine the influence of surface chemical interactions on the transport of ionic tracers in highly-weathered sediments and to illustrate the impact of these interactions on the derived transport parameters. Solute breakthrough experiments were conducted using a coarse-textured subsurface material representative of the highly weathered alluvial sediments common in the vadose zone and upper saturated zone of the Upper Coastal Plain of the southeastern U.S.A. Column studies focused on dilute tracer solutions representative of the low ionic strength pore waters and groundwaters native to these sediments.

2. Materials and methods

Sample collection and storage. Bulk material for the column study was collected on the U.S. Department of Energy's Savannah River Site which is located on the Aiken Plateau of the Upper Atlantic Coastal Plain. The vadose zone and the upper saturated zone consist mainly of red, fine to coarse sands, and clayey sands with interbeds of clay, sandy clay and gravel. To avoid bentonite contamination and sample disruption caused by conventional drilling, field moist material was collected from a deep erosional exposure of sediments representative of the vadose and upper saturated zones. The pH and electrical conductivity (EC) of the sample were determined at a 2:1 ratio (solution/sample) with deionized (DI) water, and the particle-size distribution was determined by the micro-pipette method (Miller and Miller, 1987). Triplicate samples were stirred intermittently for 30 min prior to pH and EC measurement.

X-ray diffraction. The clay fraction was dispersed by saturation with Na_2CO_3 (pH 10) and then separated by centrifugation (Jackson, 1979). Aliquots of the clay suspension were plated on petrographic slides using the Drever (1973) method, and analyzed by X-ray diffraction (XRD) from 2° to 30° (2Θ) using Cu-K_α radiation and a Philips* Norelco diffractometer equipped with a graphite monochrometer. Treatments consisted

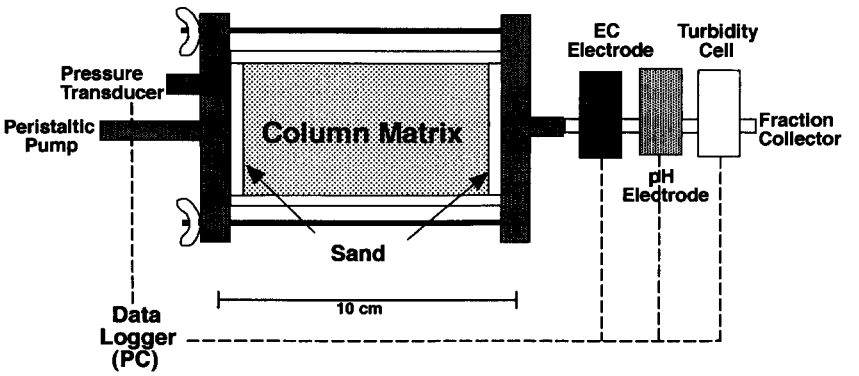

Fig. 1. Schematic diagram of experimental column setup. The pressure drop along the column and the effluent pH, turbidity and electrical conductivity (EC) were monitored continuously using a PC.

of Mg^{2+}, Mg-ethylene glycol (Mg-EG), and K^+ saturation, the latter of which was heat treated at 110°, 300° and 550°C prior to XRD analysis.

Exchangeable cations. Exchangeable cations were extracted with 0.5 *M* $BaCl_2$, and the extracts were analyzed for Na^+, Ca^{2+}, Mg^{2+}, K^+ and Al^{3+} by atomic absorption spectrometry (AAS). CEC was estimated by summing the $BaCl_2$ extractable cations.

Column experiments. The column experiments were performed in 10-cm-long Plexiglas® tubes with an interior diameter of 5 cm (Fig. 1). Field moist sample was packed in columns to a uniform density of ~ 1.5 g cm^{-3}. Columns were oriented vertically and slowly saturated from the outlet with DI water (< 0.25 mL min^{-1}). After saturation, the columns were turned horizontally and flow was initiated with a given tracer solution at a constant Darcy velocity of ~ 3.6 m day^{-1}.

The influence of various solution factors on the transport velocity of ionic solutes was observed using several different solutions. Each repacked column was used to test the breakthrough of a single solution before the matrix was replaced with fresh material. The influence of concentration and ion valance on the transport histories (i.e. behavior) of various ionic solutes was studied using 0.001–0.1 *N* solutions made from various Na^+, Ca^{2+}, Cl^- and SO_4^{2-} salts. To demonstrate how these interactions can influence the transport velocity of a commonly used "conservative" anion (Br), columns were leached with 0.001–0.1 *N* tracer solutions derived from $MgBr_2$ or KBr. In addition to the single component solutions, the influence of pH and carrier anion on the movement of mixtures of Na^+, Ca^{2+} and Mg^{2+} was investigated for a complex mixture derived from Cl^- or SO_4^{2-} salts that had been pH-adjusted over a range of 5–10. Column effluents were analyzed by AAS for Na^+, K^+, Ca^{2+}, Mg^{2+} and Al^{3+}. For comparison, tritium (~ 200 pCi mL^{-1}) was included in selected columns to calibrate the matrix pore volume. The electrical conductivity and pH of the effluent were monitored continuously, and leachate fractions were collected for cation, bromide and tritium analysis.

2.1. Bromide analysis

Effluent Br^- concentrations were determined using a bromide selective electrode (FK*1502*Br, Radiometer®) attached to a PHM *84* Research pH meter (Radiometer®) set

to measure mV. The voltage output was calibrated using a 0.1 M NaBr standard diluted over four orders of magnitude. The ionic strength of the samples and standards was adjusted by the addition of $NaNO_3$ to ensure that the ionic strength of the samples differed by $< 10\%$.

2.2. Tritium analysis

Two mL of the effluent fractions were mixed with 10 mL of scintillation cocktail and counted for 20 min (Packard Instruments Co.). Due to the low concentration of tritium in the tracer solution, effluent tracer concentrations were calibrated to various known dilutions of the inlet tracer solution.

2.3. Breakthrough analysis

Effluent tracer concentrations were plotted as maximum dimensionless concentration (C/C_0) where C_0 was the input concentration. Transport parameters V, D and R were estimated using the least-squares inversion method (CXTFIT) of Parker and van Genuchten (1984). Model 2, a deterministic linear equilibrium adsorption model consisting of one region, was calibrated to the effluent concentration data. The lack of extensive tailing for the breakthrough and leachout of tritium indicated that a one-region model was sufficient to describe the narrow distribution of flow velocities within these coarse-textured materials. Two possible cases were evaluated for each set of breakthrough curves (BTC's): (a) the retardation factor (R) for the solute of interest was assumed to be 1 (no interaction) and the pore water velocity was estimated by the model; and (b) the pore water velocity ($V = q/\theta$) was estimated from the inlet flux and the volumetric water content of the column, and R was estimated by the model. In both cases the model was allowed to estimate D. Because two adjustable parameters were fitted in each case, the resulting r^2 and predicted BTC were identical. The volumetric water content (θ) was assumed to be equivalent to the column porosity because of the coarse texture of the column matrix. Assuming a particle density (ρ_p) of 2.65 g cm^{-3}, the total column porosity was estimated from the bulk density (ρ_b) and total volume for each repacked column (Danielson and Sutherland, 1986).

3. Results and discussion

3.1. Sample characteristics

The particle size distribution of the sandy subsurface material was consistent with that observed throughout the upper saturated zone ($< 10\%$ clay) with very little silt present. The clay fraction, as determined by XRD, consisted primarily of kaolinite, goethite and mica (illite) while the coarse fraction (> 2 μm) was almost exclusively quartz. CEC of the bulk material, estimated from the total sum of Ba^{2+} extractable cations, was extremely low (0.625 cmol(+) kg^{-1}), with a major portion of the exchange complex occupied by exchangeable Al^{3+} ($\sim 85\%$) (Table 1).

Table 1
Physical and chemical characteristics of the sample used in the column experiments

Cation [a]	cmol(+) kg^{-1} ($\times 10^3$)	SD [b] ($\times 10^3$)
Na	2.4	0.4
Ca	14.7	1.2
Mg	72.1	6.7
K	5.8	0.6
Al	530	63.8
CEC [c]	625	72.4
ESP [d]	0.38	0.03
Extractable Al (%)	84.8	0.37
	g/100 g	SD [b]
Sand	90.6	1.3
Silt	1.3	1.3
Clay	8.2	2.0
pH data		
pH (water)	4.94	0.04
pH (KCl)	4.42	0.07
EC (μS cm^{-1}) 2:1 mixture	5.47	0.49

[a] Extractable in 1 *N* $BaCl_2$.
[b] Standard deviation.
[c] Sum of extractable cations.
[d] Exchangeable sodium percentage.

3.2. *Breakthrough of 0.001 N salts* (Fig. 2A)

Initially, EC was used as an estimate of breakthrough for the various salt solutions. Though EC is insensitive to ionic identity, it represents the most conservative estimate of the possible inlet solute breakthrough under conditions where the tracer solution was significantly higher in ionic solutes than the initial pore water (i.e., $1 \leq R_{EC} \leq R_{inlet\ solutes}$). If solute transport was occurring by piston flow, the leaching front of a conservative tracer should show an immediate breakthrough that coincides with one pore volume. Tritium breakthrough was consistent with pore volume estimates based on the column bulk density (Fig. 2A). However, the obvious delay of ionic solutes with respect to the breakthrough of tritium confirms that both treatment solution cations and anions were retarded, and the degree of retardation was dependent on the identity of the treatment solution cation and anion, indicating that both the apparent anion- and cation-exchange capacity were sensitive to solution conditions. If simple equivalent exchange was occurring within the column, native cations and anions should be released into solution in equivalent concentrations to those retained; thus, the breakthrough of EC would still coincide with that of tritium, even though the actual composition of the

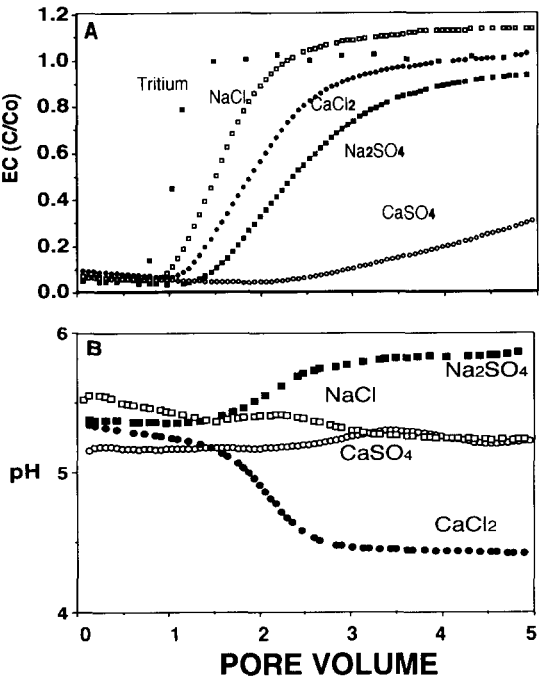

Fig. 2. Effluent pH (B) and EC (A) breakthrough for various 0.001 *N* salt solutions.

solution may have changed dramatically. Of the 0.001 *N* solutions tested, NaCl yielded the most conservative breakthrough, but was still significantly retarded compared to tritium. Calcium chloride eluted next, followed by Na_2SO_4, and finally $CaSO_4$. If the 0.001 *N* solutes were considered to be conservative ($R = 1$), at least in terms of equivalent exchange, the volumetric water content estimated by CXTFIT (Table 2) ranged from 0.64 to the physically unrealistic value of 2.66, dramatically different from the values based on bulk density or tritium breakthrough.

Even though the Al^{3+} concentration in the column effluent was below the detection limit for flame AAS, the degree of retardation observed for the various salt solutions and the effluent pH trends suggest that exchangeable Al^{3+} was playing a major role in buffering the pH of the system and in controlling the solute migration behavior. Exchangeable aluminum combined with oxide surfaces can act as "apparently" nonequivalent sinks for both solution cations and anions:

$$\underset{\text{cation ex. sites}}{Al^{3+}} + \tfrac{3}{2}Ca^{2+} \rightarrow \underset{\text{cation ex. sites}}{\tfrac{3}{2}Ca^{2+}} + Al(OH)_m^{3-m} + mH^+ \qquad (5)$$

After exchange with treatment solution cations, aluminum hydrolysis reactions reduce the equivalency of the exchanged Al^{3+} species and generate acidity that buffers the pH in favor of continued anion sorption. However, re-adsorption of Al^{3+} hydrolysis

Table 2
Column parameters estimated with model 2 of CXTFIT (Parker and van Genuchten, 1984)

	Estimated V [a] (cm min^{-1})	CXTFIT V [a] (cm min^{-1})	D [b] (cm^2 min^{-1})	Dispersivity (cm)	R [c]	Volumetric water content CXTFIT θ	estimated θ	r^2
0.001 N salt breakthrough (Fig. 2):								
NaCl	0.59	0.4	0.15	0.37	–	0.64	0.43	1.00
	0.59	–	0.22	0.38	1.44		0.43	1.00
Ca-chloride	0.59	0.31	0.18	0.60	–	0.83	0.43	1.00
	0.59	–	0.36	0.60	1.92		0.43	1.00
Na-sulfate	0.60	0.23	0.21	0.88	–	1.09	0.43	1.00
	0.60	–	0.53	0.88	2.55		0.43	1.00
Ca-sulfate	0.60	0.1	0.08	0.85	–	2.66	0.43	0.99
	0.60	–	0.53	0.88	5.75		0.43	0.99
0.100 N salt breakthrough (Fig. 3):								
NaCl	0.60	0.58	0.25	0.43	–	0.44	0.43	1.00
	0.60	–	0.25	0.43	1.03		0.43	1.00
Ca-chloride	0.60	0.58	0.09	0.16	–	0.44	0.43	1.00
	0.60	–	0.10	0.16	1.04		0.43	1.00
Na-sulfate	0.60	0.54	0.13	0.24	–	0.47	0.42	0.95
	0.60	–	0.14	0.24	1.12		0.42	0.95
Influence of ionic strength on Br breakthrough (Fig. 5):								
0.001 *N*	0.60	0.29	0.13	0.47	–	0.89	0.42	0.99
	0.60	–	0.28	0.47	2.1		0.42	0.99
0.01 *N*	0.60	0.45	0.23	0.50	–	0.56	0.42	1.00
	0.60	–	0.30	0.50	1.31		0.42	1.00
0.1 *N*	0.63	0.56	0.27	0.47	–	0.45	0.41	1.00
	0.63	–	0.30	0.48	1.16		0.41	1.00

[a] Pore water velocity.
[b] Hydrodynamic dispersion coefficient.
[c] Retardation factor.

products, especially on kaolinite (Hodges and Zelazny, 1983), make it difficult to perform charge and mass balance estimates based on the composition of column effluents (Parker et al., 1979; Seaman et al., 1995).

$$\equiv FeOH + H^+ \rightarrow \equiv FeOH_2^+ \ A^- \tag{6}$$

In the absence of a source of acidity [reaction (5)], net adsorption of anions on variable-charge oxide surfaces should result in a shift in pH towards the ZPC of the sorbing mineral (Uehara and Gillman, 1981) [reaction (6)]. Therefore, anion adsorption by variable-charge surfaces in the column system consumes acidity generated by Al exchange and hydrolysis, with the coupling of these two reactions between the different

surfaces resulting in a greater net-cation and anion adsorption than would occur by either reaction alone.

Despite the obvious differences in retardation, NaCl and $CaSO_4$ solutions resulted in approximately the same effluent pH histories (Fig. 2B), which changed little during the course of leaching and reflected similar preferences of the two reactions for both cation–anion pairs (Uehara and Gillman, 1981). For the NaCl solution, neither ion was capable of displacing surface forms of acidity or alkalinity and the solution pH remained essentially unchanged. In the case of the $CaSO_4$ solution, the two ions were approximately equal in their ability to displace surface acidity and alkalinity; exchangeable Al^{3+} and protons in the case of Ca^{2+} and surface hydroxyls in the case of SO_4^{2-}. The presence of SO_4^{2-}, an anion with a higher affinity for the oxide surface than Cl^-, tends to increase solution pH by displacing hydroxyls from oxyhydroxide surfaces (Hohl et al., 1980), which neutralizes aluminum or surface protons exchanged by Ca^{2+}. In the case of the Na_2SO_4 solution, SO_4^{2-} was effective at displacing surface hydroxyls, whereas the Na^+ was ineffective at displacing Al^{3+}, thus increasing effluent pH (Nye et al., 1961).

3.3. Breakthrough of 0.100 N salts

When the equivalent concentration of the treatment solutions was raised to 0.1 *N*, the identity of the cation and anion had little influence on the EC breakthrough (Fig. 3A)

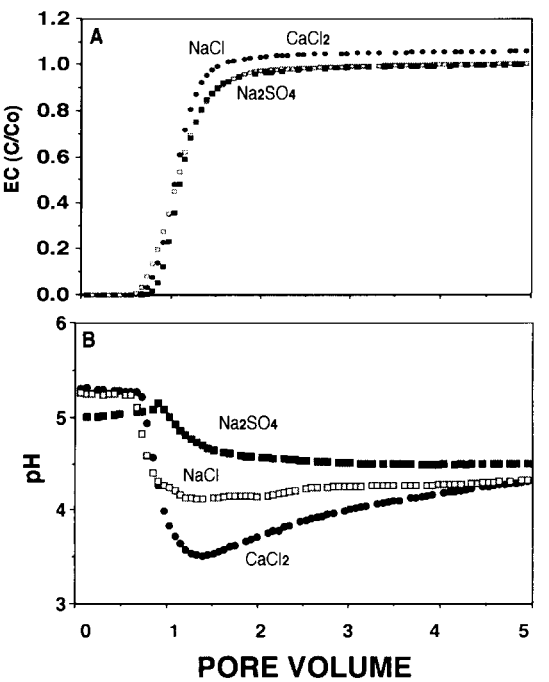

Fig. 3. Effluent pH (B) and EC (A) breakthrough for various 0.1 *N* salt solutions.

and the two estimates of θ were consistent (Table 2). In other words, at the point when the anion begins to act conservatively the entire solution, in terms of net equivalents, functions conservatively with respect to EC breakthrough. To some degree this is a function of the coarse texture of the matrix and the requirement for maintaining electrical neutrality within the column, but it illustrates that any solute can be used as a conservative tracer if its concentration greatly exceeds the adsorption capacity of the matrix. It is important to note that even the 0.001 *N* solutions are several times more concentrated than native groundwater of this region (Strom and Kaback, 1992).

As observed at the lower ionic strengths, the effluent pH results from a balance between anion adsorption on the oxide surface that tends to increase the pH, and cation exchange and Al hydrolysis that tend to lower the pH. When the anion adsorption capacity of the matrix was exceeded at the higher concentrations, the effluent pH was dominated by the reactions of Al exchange and hydrolysis; thus, a decrease in pH was observed regardless of cation or anion valence. However, the relative order with respect to effluent pH was consistent with the ability of the treatment cation to replace exchangeable Al and the sorption preferences for the treatment anions that were observed at lower ionic strengths.

3.4. Influence of anions on cation selectivity

Mixed-cation solutions (250 mg L^{-1} Na^+, 15 mg L^{-1} Mg^{2+}, 5 mg L^{-1} Ca^{2+}) prepared from either sulfate or chloride salts were pH-adjusted over the range of 5.6–10.0 prior to conducting leaching experiments (Fig. 4). Transport behavior of these mixed-cation solutions illustrates the sensitivity of this system to mild changes in solute composition. At the high inlet concentration, sodium displayed the most conservative transport behavior of the three cations, but was delayed to a greater extent in the presence of sulfate and with increasing pH (Fig. 4B). The impact of solution pH and anion valance was even more dramatic for the transport of divalent cations, Ca^{2+} and Mg^{2+}. In the presence of chloride, Mg^{2+} was concentrated in the initial effluent due to competition with Ca^{2+} for exchange sites and the release of native Mg^{2+} from the exchange complex (Fig. 4A). This was much less evident at the higher pH regimes and Mg^{2+} became only slightly elevated compared to the inlet concentration. With prolonged leaching of the high-pH solution, the effluent Mg^{2+} concentration actually decreased to about half of that of the inlet solution, reflecting an increase in Mg^{2+} adsorption and the "effective" CEC of the column matrix when leached with the alkaline treatment solution, even though the effluent pH was the same as the pH 5.6 solution treatment. Calcium displayed the highest degree of retardation that increased with increasing inlet pH.

When the inlet solutions were comprised of sulfate salts, the breakthrough of Mg^{2+} and Ca^{2+} was dramatically different from that of chloride salts (Fig. 4B). The transport of Mg^{2+} was retarded to a greater extent, and the concentration failed to surpass the inlet concentration until ~ 6 pore volumes had been passed though the column. At the higher pH, the Mg^{2+} concentration was never higher than the inlet concentration during the first 10 pore volumes of leaching. Calcium was delayed to a greater extent in the presence of sulfate and the degree of retardation increased at higher influent pH-values.

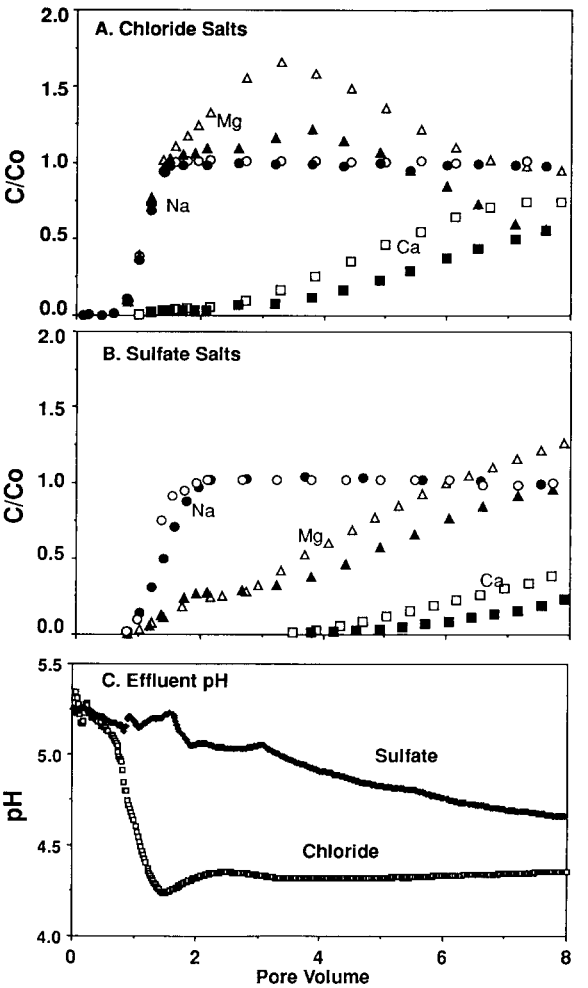

Fig. 4. Relative cation breakthrough (C/C_0) for mixed cation solutions (250 mg L^{-1} Na, 15 mg L^{-1} Ca, 5 mg L^{-1} Mg) prepared from: (A) chloride salt; and (B) sulfate salt. *Open symbols* refer to solutions with a pH of 5.6 and *closed symbols* refer to solutions with an adjusted pH of 10. The resulting effluent pH (C) for sulfate and chloride solutions (inlet pH ~ 5.6).

The effluent pH of the column was more dependent on the treatment anion than on the pH of the inlet solution, illustrating the influence of the anion on surface chemical reactions controlling the buffering capacity of the aquifer sediments (Fig. 4C). The same approximate effluent pH was observed regardless of the influent pH of a given anion treatment. The decrease in pH observed for the chloride solutions was not observed for the sulfate treatments because of the greater ability of the sulfate ligand to exchange for surface hydroxyls present on the variable-charge surfaces, thus buffering the solution

against acidity generated either by specific adsorption of treatment cations or Al^{3+} exchange and hydrolysis (Alva et al., 1991). Even though the same effluent pH was observed for all solutions derived from a given anion, the higher-pH inlet solutions appear to be effective at generating CEC within the column through a combination of increasing the net-negative charge on oxides and neutralizing exchangeable Al^{3+}. The effluent solution pH for the sulfate treatment approached that of the chloride solution with continued leaching and may reflect a limit to the ability of the sulfate interaction with the oxide surface to counter any downward shift in pH caused by Al^{3+} hydrolysis.

The increase in retardation of treatment cations in the presence of sulfate has been attributed to the increase in pH and surface negative charge that accompanies sulfate adsorption on variable-charge minerals such as Fe-oxides (Bolan et al., 1993). Wann and Uehara (1978a, 1978b) observed that the affinity of an oxidic soil for Ca^{2+} and Mg^{2+} increased with increasing levels of applied phosphate. In addition to these mechanisms, co-adsorption of the cation and anion has been suggested to increase cation retention in the presence of sulfate (Marcano-Martinez and McBride, 1989; Alva et al., 1991).

3.5. Br breakthrough

The influence of solution composition on the breakthrough of ionic species was also illustrated in the retardation of Br^-. Estimates of pore volume based on tritium breakthrough were consistent with those based on bulk density and typically differed by $< 5\%$. At higher concentrations (1.0–0.1 *M*), the breakthrough was essentially unaffected by Br^- concentration and the valance of the carrier cation (Fig. 5). At concentrations below 0.1 *M*, breakthrough was dependent on both the concentration of the tracer solution and on the valence of the carrier cation. Retardation factors for Br^- ranged from a low of 1.16 for 0.1 *N* KBr to 2.10 for 0.001 *N* KBr; however, the low-ionic-strength solutions of $MgBr_2$ displayed the greatest delay in breakthrough. The increased retardation of Br^- in the presence of Mg^{2+} may be due in part to the adsorption of the polyvalent cation to the oxide surfaces at pH-values below the oxide ZPC (Kinniburgh et al., 1975, 1976), resulting in a decrease in solution pH and an increase in net positive surface charge (Bleam and McBride, 1984). In addition, the greater ability of Mg^{2+} compared to K^+ to exchange with Al^{3+} would tend to lower the solution pH and thus increase the net-positive charge on the Fe-oxide surface. Although the BTC's differ in shape for the two acid-washed sand columns (Fig. 5B), Br^- derived estimates of porosity were independent of ionic strength or carrier cation (not shown) and consistent with those based on the bulk density of the column matrix.

The influence of ionic strength and counter ion valance on anion retardation can be explained by the Gouy–Chapman diffuse double layer model of surface charge. Under conditions of constant pH, the surface charge of a variable-charge mineral is proportional to the square root of the concentration of an indifferent electrolyte, in this case the tracer solution (Uehara and Gillman, 1981). Even though this predicts that the number of anion adsorption sites for a mineral below its ZPC will increase with increasing concentration of the tracer, the total percentage of the inlet solution anions adsorbed for a given ionic strength decreases dramatically as the concentration is increased. Regard-

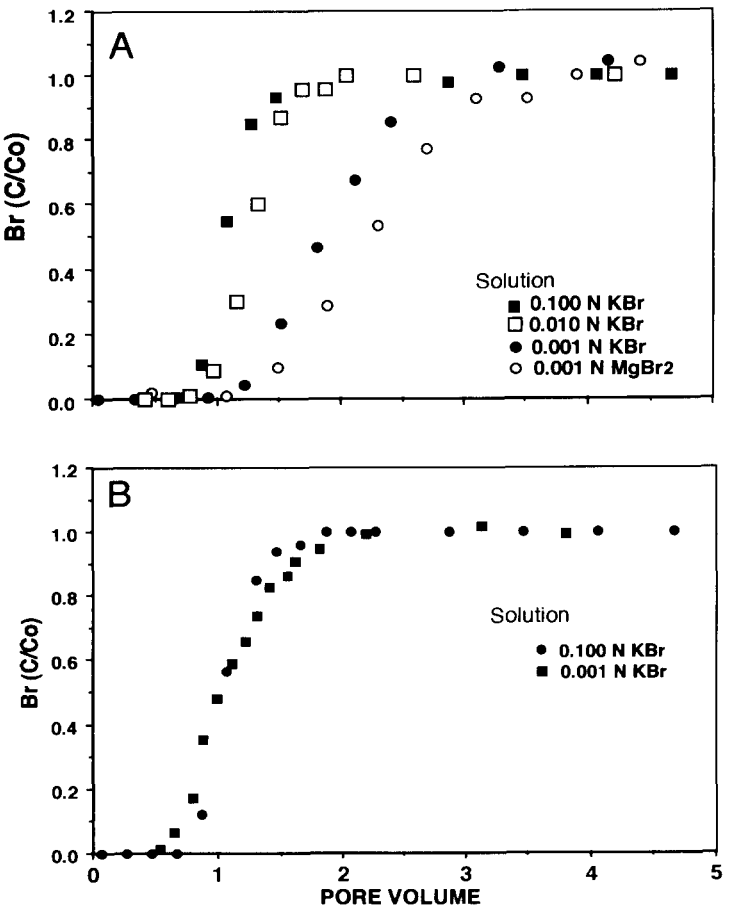

Fig. 5. Bromide breakthrough in the coarse textured sediments (A) and acid-washed sand (B). (A) shows the influence of concentration and cation valence on Br breakthrough.

less of the proposed mechanism for ion retardation, the adsorbed ion will approach conservative behavior as its concentration exceeds the adsorption capacity of the matrix and the ability to experimentally detect minute degrees of retardation; conversely, retardation will increase dramatically if the inlet concentration is low relative to the sorption capacity of the matrix.

4. Conclusions

The simultaneous retardation of both cations and anions without an obvious exchange for native ionic species suggests not only a heterogeneity with respect to surface charge and adsorption sites, but also an adsorption mechanism that would tend to generate

roughly equivalent cation and anion sorption sites within the aquifer matrix. This surface–solute interaction often referred to as "salt sorption" has been widely observed in batch adsorption studies of highly weathered soils, but it may not be easily recognized in solute transport experiments because of the tendency to focus on the fate of a particular cation or anion and neglect the influence or fate of the counter ion.

Several possible mechanisms can be invoked to account for the simultaneous retardation of both cations and anions without an obvious exchange for native species, but experimentally distinguishing between these mechanisms or combinations of these mechanisms based on bulk solution data in complex systems containing several types of surfaces may be difficult, if not impossible. Anion retardation is usually attributed to adsorption on the Fe- and Al-oxide fraction, but the simple model of adsorption on a single variable-charge surface such as goethite, was inadequate to describe the observed shifts in effluent pH and both cation and anion transport behavior. Wada (1984) attributed the increase in cation- and anion-exchange capacity of andisols to the ionic strength charging of variable-charge surfaces with differing zero point of charges (ZPC's). When batch adsorption experiments were conducted with separate phases, Wada (1984) observed that an increase in concentration and adsorption of either the anion, in the case of aluminum hydroxide, or the cation in the case of silica, resulted in a shift in the solution pH towards the ZPC of the sorbing phase. If the two solid phases were combined, the shift in solution pH for each of the surfaces was neutralized by the adsorption reaction of the other surface.

The highly weathered sediments studied here generally display the same type of behavior described by Wada (1984) for adsorption on a combination of surfaces with differing ZPC's, but several observations indicate that Al^{3+} exchange and hydrolysis may play an important role in controlling adsorption and transport of ionic solutes. Even though silica has a low ZPC (pH $\sim$ 2.0) and can act as a variable-charge adsorption site for cations at the pH of the present study, the coarse texture and low reactive surface area make it unlikely that the quartz sand fraction can account for the cation adsorption observed in the column experiments (Fig. 5B). In batch adsorption experiments "salt sorption" is often accompanied by a reduction in neutral salt extractable Al^{3+} (exchangeable Al) (Pearce, 1994). Exchangeable aluminum can act as a sink for both solution cations and hydroxyls generated during adsorption of tracer anions on variable-charge surfaces, thus countering any shift in the solution pH that accompanies anion adsorption and reduces the exchange equivalency of the Al^{3+} species. When the anion adsorption potential within the matrix was exceeded at high ionic strengths, Al exchange and hydrolysis continued and a decrease in pH was observed regardless of the treatment solution anion.

The results of this study suggest that highly-weathered sediments should be viewed as mixed variable/constant charge systems that are at, or very near their zero point of net charge (ZPNC). Therefore, both the sign and magnitude of surface charge are sensitive to changes in solution composition, i.e. cation/anion type, pH and ionic strength. In one-dimensional column experiments, reliable independent estimates of basic model parameters such as flow rate and porosity make the recognition of non-conservative behavior more straightforward, but at the field scale it may be impossible to distinguish between adsorption reactions and the physical parameters that the experiment may be

attempting to characterize. Based on breakthrough curves (BTC's), chemical interactions such as adsorption, ion exchange and even exclusion may be interpreted as having a physical significance (i.e. mixing, flow rate, permeability, immobile/mobile regions, etc.). If the transport of an adsorbed ionic species is assumed to be conservative ($R = 1$), calibration of the advection–dispersion model of solute transport would underestimate flow velocity or overestimate formation porosity. It is easy to visualize that a pulse of tracer solutes would demonstrate extreme "non-conservative" behavior as dilution and hydrodynamic dispersion are combined with the ionic strength dependent adsorption of the tracer as it moved through the region of interest, thus negating the validity of derived transport parameters.

Acknowledgements

This research was performed for the Westinghouse Savannah River Company under control contract No. AA 71883V and also partially funded by contract DE-AC09-76SROO-819 between the University of Georgia and the U.S. Department of Energy. The authors would like to acknowledge the thoughtful comments of Drs. R. Dasika, S.F. Korom and C. Strojan on an early version of the manuscript, and the technical assistance of R. Arnold, B. Pidcoe, Dr. R. Strom and R. Winkler.

References

Alva, A.K., Sumner, M.E. and Miller, W.P., 1991. Salt adsorption in gypsum amended acid soils. In: Plant–Soil Interactions at Low pH. Kluwer, Dordrecht, pp. 93–97.

Berg, W.A. and Thomas, G.W., 1959. Anion elution patterns from soils and soil clays. Soil Sci. Soc. Am. Proc., 23: 348–350.

Bleam, W.F. and McBride, M.B., 1984. Cluster formation versus isolated-site adsorption — A study of Mn(II) and Mg(II) adsorption on boehmite and goethite. J. Colloid Interface Sci., 103: 124–132.

Boggs, J.M. and Adams, E.E., 1992. Field study of dispersion in a heterogeneous aquifer, 4. Investigation of adsorption and sampling bias. Water Resour. Res., 28: 3325–3336.

Bolan, N.S., Syers, J.K. and Sumner, M.E., 1993. Calcium-induced sulfate adsorption by soils. Soil Sci. Soc. Am. J., 57: 691–696.

Cameron, K.C. and Wild, A., 1982. Comparative leaching of chloride, nitrate and tritiated water under field conditions. J. Soil Sci., 33: 649–657.

Chan, K.Y., Geering, H.R. and Davey, B.G., 1980. Movement of chloride in a soil with variable charge properties, I. Chloride systems. J. Environ. Qual., 9: 579–582.

Danielson, R.E. and Sutherland, P.L., 1986. Porosity. In: A. Klute (Editor), Methods of Soil Analysis, Part 1. Soil Sci. Soc. Am., Madison, WI, pp. 443–461.

Drever, J.I., 1973. The preparation of oriented clay mineral specimens for X-ray diffraction analysis by a filter membrane peel technique. Am. Mineral., 58: 553–554.

Freyberg, D.L., 1986. A Natural gradient experiment on solute transport in a sand aquifer, 2. Spatial moments and the advection and dispersion of nonreactive tracers. Water Resour. Res., 22: 2031–2046.

Gelhar, L.W., Welty, C. and Rehfeldt, K.R., 1992. A critical review of data on field-scale dispersion in aquifers. Water Resour. Res., 28: 1955–1974.

Hodges, S.C. and Zelazny, L.W., 1983. Influence of OH/Al ratios and loading rates on aluminum–kaolinite interactions. Soil Sci. Soc. Am. J., 47: 221–225.

Hohl, H., Sigg, L. and Stumm, W., 1980. Characterization of surface chemical properties of oxides in natural waters — The role of specific adsorption in determining the surface charge. In: M.C. Kavanaugh and J.O. Leckie (Editors), Particles in Water: Characterization, Fate, Effects, and Removal. Am. Chem. Soc., Washington, DC, pp. 3–29.

Ishiguro, M., Song, K.C. and Yuita, K., 1992. Ion Transport in an Allophanic Andisol under the influence of variable charge. Soil Sci. Soc. Am. J., 56: 1789–1793.

Jackson, M.L., 1979. Soil Chemical Analysis — Advanced Course. Published by the author, Dep. Soil Sci., Univ. of Wisconsin, Madison, WI, 2nd ed., 9th printing, 895 pp.

Jensen, K.H., Bitsch, K. and Bjerg, P.L., 1993. Large-scale dispersion experiments in a sandy aquifer in Denmark: Observed tracer movements and numerical analyses. Water Resour. Res., 29: 673–696.

Kinniburgh, D.G., Syers, J.K. and Jackson, M.L., 1975. Specific adsorption of trace amounts of calcium and strontium by hydrous oxides of iron and aluminum. Soil Sci. Soc. Am. Proc., 39: 464–470.

Kinniburgh, D.G., Jackson, M.L. and Syers, J.K., 1976. Adsorption of alkaline earth, transition, and heavy metal cations by hydrous oxide gels of iron and aluminum. Soil Sci. Soc. Am. Proc., 40: 796–799.

Marcano-Martinez, E. and McBride, M.B., 1989. Calcium and sulfate retention by two oxisols of the Brazilian Cerrado. Soil Sci. Soc. Am. J., 53: 63–69

McMahon, M.A. and Thomas, G.W., 1974. Chloride and tritium flow in disturbed and undisturbed soil cores. Soil Sci. Soc. Am. Proc., 38: 727–732.

Miller, W.P. and Miller, D.M., 1987. A micro-pipette method for soil mechanical analysis. Commun. Soil Sci. Plant Anal., 18: 1–15.

Nye, P., Craig, D., Coleman, N.T. and Ragland, J.L., 1961. Ion exchange equilibrium involving aluminum. Soil Sci. Soc. Am. Proc., 25: 14–17.

Parker, J.C. and van Genuchten, M.Th., 1984. Determining transport parameters from laboratory and field tracer experiments. Va. Polytech. Inst., Va. Agric. Exp. Stn., Blacksburg, VA, Bull. No. 84-3.

Parker, J.C., Zelazny, L.W., Sampath, S. and Harris, W.G., 1979. A critical evaluation of the extension of zero point of charge (ZPC) theory to soil systems. Soil Sci. Soc. Am. J., 43: 668–674.

Pearce, R.C., 1994. Investigation of salt sorption behavior by acid soils and synthetic goethite. Ph.D. Dissertation, University of Georgia, Athens, GA.

Seaman, J.C., Bertsch, P.M. and Miller, W.P., 1995. Chemical controls on colloid generation and transport in a sandy aquifer. Environ. Sci. Technol., 29: 1808–1814.

Sposito, G., 1984. The Surface Chemistry of Soils. Oxford University Press, New York, NY.

Strom, R.N. and Kaback, D.S., 1992. SRS baseline hydrogeologic investigation: aquifer characterization: Groundwater chemistry of the Savannah River Site and vicinity. Westinghouse Savannah River Co., Aiken, SC, WSRC-RP-92-450.

Stumm, W. and Morgan, J.J., 1981. Aquatic Chemistry: An Introduction Emphasizing Chemical Equilibria in Natural Waters. Wiley–Interscience, New York, NY, 2nd ed.

Thomas, G.W. and Swoboda, A.R., 1970. Anion exclusion effects on chloride movement in soils. Soil Sci., 110: 163–166.

Uehara, G. and Gillman, G., 1981. The mineralogy, chemistry, and physics of tropical soil with variable charge clays. Westview Tropical Agriculture Series, No. 4. Westview, Boulder, CO.

van Olphen, H., 1977. An Introduction to Clay Colloid Chemistry. Wiley–Interscience, New York, NY, 2nd ed.

Wada, S., 1984. Mechanism of apparent salt adsorption in ando soils. Soil Sci. Plant Nutr., 30: 77–83.

Wann, S.S. and Uehara, G., 1978a. Surface charge manipulation of constant surface potential soil colloids, I. Relation to sorbed phosphorus. Soil Sci. Soc. Am. J., 42: 565–570.

Wann, S.S. and Uehara, G., 1978b. Surface charge manipulation of constant surface potential soil colloids, II. Effect on solute transport. Soil Sci. Soc. Am. J., 42: 886–888.

Wong, M.T.F., Hughes, R. and Rowell, D.L., 1990. Retarded leaching of nitrate in acid soils from the tropics: measurement of the effective anion exchange capacity. J. Soil Sci., 41: 655–663.